Inorg. Chem. **2008**, *47*, 9380−9389

Thermodynamic and Kinetic Studies of H Atom Transfer from $HMo(CO)_3(\eta^5\text{-}C_5H_5)$ to $Mo(N[t\text{-}Bu]Ar)_3$ and $(PhCN)Mo(N[t\text{-}Bu]Ar)_3$: Direct Insertion of Benzonitrile into the Mo−H Bond of $HMo(N[t\text{-}Bu]Ar)_3$ forming $(Ph(H)C{=}N)Mo(N[t\text{-}Bu]Ar)_3$

Manuel Temprado,[†,‡] James Eric McDonough,[§] Arjun Mendiratta,[†] Yi-Chou Tsai,[†,||] George C. Fortman,[§] Christopher C. Cummins,*[,†] Elena V. Rybak-Akimova,*[,‡] and Carl D. Hoff*[,§]

Department of Chemistry, Massachusetts Institute of Technology, 77 Massachusetts Avenue, Cambridge, Massachusetts 02139, Department of Chemistry, Tufts University, 62 Talbot Avenue, Medford, Massachusetts, 02155, and Department of Chemistry, University of Miami, 1301 Memorial Drive, Coral Gables, Florida, 33146

Received May 25, 2008

Synthetic studies are reported that show that the reaction of either H_2SnR_2 (R = Ph, *n*-Bu) or $HMo(CO)_3(Cp)$ (**1**-H, Cp = η^5-C_5H_5) with $Mo(N[t\text{-}Bu]Ar)_3$ (**2**, Ar = 3,5-$C_6H_3Me_2$) produce $HMo(N[t\text{-}Bu]Ar)_3$ (**2**-H). The benzonitrile adduct $(PhCN)Mo(N[t\text{-}Bu]Ar)_3$ (**2**-NCPh) reacts rapidly with H_2SnR_2 or **1**-H to produce the ketimide complex $(Ph(H)C{=}N)Mo(N[t\text{-}Bu]Ar)_3$ (**2**-NC(H)Ph). The X-ray crystal structures of both **2**-H and **2**-NC(H)Ph are reported. The enthalpy of reaction of **1**-H and **2** in toluene solution has been measured by solution calorimetry ($\Delta H = -13.1 \pm 0.7$ kcal mol^{-1}) and used to estimate the Mo−H bond dissociation enthalpy (BDE) in **2**-H as 62 kcal mol^{-1}. The enthalpy of reaction of **1**-H and **2**-NCPh in toluene solution was determined calorimetrically as $\Delta H = -35.1 \pm 2.1$ kcal mol^{-1}. This value combined with the enthalpy of hydrogenation of $[Mo(CO)_3(Cp)]_2$ (**1**$_2$) gives an estimated value of 90 kcal mol^{-1} for the BDE of the ketimide C−H of **2**-NC(H)Ph. These data led to the prediction that formation of **2**-NC(H)Ph via nitrile insertion into **2**-H would be exothermic by ∼36 kcal mol^{-1}, and this reaction was observed experimentally. Stopped flow kinetic studies of the rapid reaction of **1**-H with **2**-NCPh yielded $\Delta H^{\ddagger} = 11.9 \pm 0.4$ kcal mol^{-1}, $\Delta S^{\ddagger} = -2.7 \pm 1.2$ cal K^{-1} mol^{-1}. Corresponding studies with $DMo(CO)_3(Cp)$ (**1**-D) showed a normal kinetic isotope effect with $k_H/k_D \approx 1.6$, $\Delta H^{\ddagger} = 13.1 \pm 0.4$ kcal mol^{-1} and $\Delta S^{\ddagger} = 1.1 \pm 1.6$ cal K^{-1} mol^{-1}. Spectroscopic studies of the much slower reaction of **1**-H and **2** yielding **2**-H and $^1/_2$**1**$_2$ showed generation of variable amounts of a complex proposed to be $(Ar[t\text{-}Bu]N)_3Mo{-}Mo(CO)_3(Cp)$ (**1**−**2**). Complex **1**−**2** can also be formed in small equilibrium amounts by direct reaction of excess **2** and **1**$_2$. The presence of **1**−**2** complicates the kinetic picture; however, in the presence of excess **2**, the second-order rate constant for H atom transfer from **1**-H has been measured: 0.09 ± 0.01 M^{-1} s^{-1} at 1.3 °C and 0.26 ± 0.04 M^{-1} s^{-1} at 17 °C. Study of the rate of reaction of **1**-D yielded $k_H/k_D = 1.00 \pm 0.05$ consistent with an early transition state in which formation of the adduct $(Ar[t\text{-}Bu]N)_3Mo\cdots HMo(CO)_3(Cp)$ is rate limiting.

Introduction

The addition of benzonitrile to $Mo(N[t\text{-}Bu]Ar)_3$ (**2**, Ar = 3,5-$C_6H_3Me_2$) results in the formation of equilibrium amounts of $(PhCN)Mo(N[t\text{-}Bu]Ar)_3$ (**2**-NCPh), which reacts rapidly with X_2 (X = SC_6H_5, SC_6F_5, SeC_6H_5, TeC_6H_5, OC(O)Ph) to form substituted ketimide complexes of general form $(Ph(X)C{=}N)Mo(N[t\text{-}Bu]Ar)_3$. Some of these complexes undergo clean extrusion of nitrile to form $XMo(N[t\text{-}Bu]Ar)_3$. Known thermodynamic parameters corresponding to such reactions are summarized in the thermochemical cycle in Scheme 1 showing that nitrile extrusion is exothermic only for X = OC(O)Ph and that the driving force for this reaction is primarily entropic for the other complexes studied.[1] These data suggest that the reverse of the β-X elimination reaction, nitrile insertion, should be favorable for suitable X groups.

Lending credence to this hypothesis is the observation that $Nb(H)(\eta^2\text{-}t\text{-}Bu(H)C{=}NAr)(N[CH_2\text{-}t\text{-}Bu]Ar)_2$, which is the

* To whom correspondence should be addressed. E-mail: ccummins@mit.edu (C.C.C.), erybakak@tufts.edu (E.V.R.-A), c.hoff@miami.edu (C.D.H).
† Massachusetts Institute of Technology.
‡ Tufts University.
§ University of Miami.
|| Current address: Department of Chemistry, National Tsing Hua University, Hsinchu 30013, Taiwan, Republic of China.

10.1021/ic800945m CCC: $40.75
Published on Web 09/13/2008

Scheme 1. Thermodynamic Data for Enthalpies of Reaction (kcal mol^{-1}) for the Assembly of Ketimide Complexes and for Nitrile Extrusion Reactions

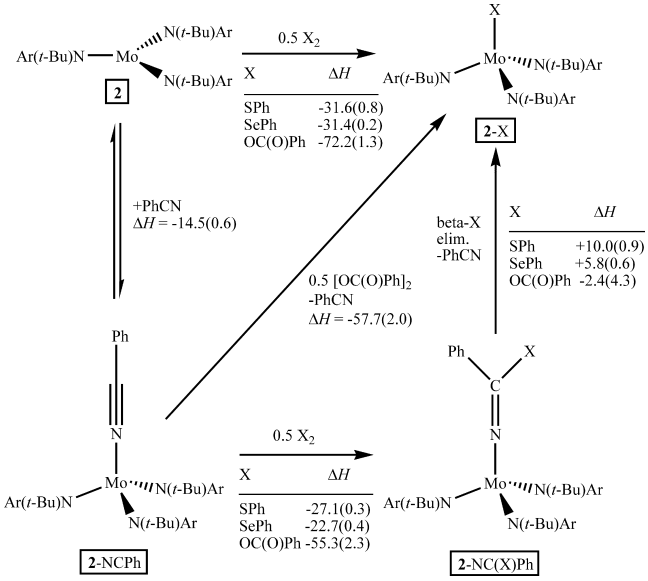

C−H oxidative addition form of the trisamide species $Nb(N[CH_2\text{-}t\text{-}Bu]Ar)_3$, reacts with mesityl nitrile to form η^2-(MesCN)$Nb(N[CH_2\text{-}t\text{-}Bu]Ar)_3$, whereas reaction with *t*-BuCN results in insertion of the nitrile into the Nb−H bond forming the ketimide complex $(H(t\text{-}Bu)C{=}N)Nb(\eta^2\text{-}t\text{-}Bu(H)C{=}NAr)(N[CH_2\text{-}t\text{-}Bu]Ar)_2$.[2]

Legzdins and co-workers[3] have reported direct insertion of acetonitrile into the W−H bond of the 16-valence electron complex $(\eta^5\text{-}C_5Me_5)W(NO)(CH_2SiMe_3)H$ forming $(\eta^5\text{-}C_5Me_5)W(NO)(CH_2SiMe_3)(N{=}C(H)CH_3)$; however, there are relatively few reports of nitrile insertion into metal−hydride or metal−alkyl bonds in transition-metal complexes. Recent studies of nitrile insertion into lanthanide and actinide complex bonds have been reported,[4] such as that shown for the thorium (and the uranium analog) complexes in eq 1.

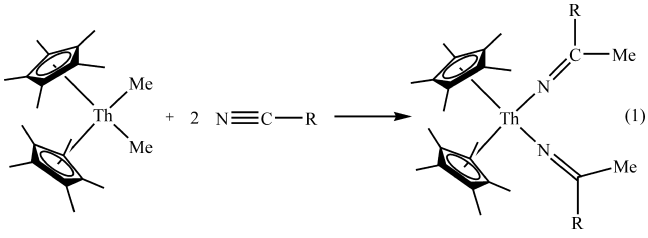

(1)

The present work reports synthetic, thermodynamic, and kinetic studies relevant to reactions shown in Scheme 1, for X = H. In this case, it is shown that nitrile insertion, rather than extrusion, is the thermodynamically favored and observed reaction.

Experimental Section

General Considerations. Unless stated otherwise, all operations were performed in a Vacuum Atmospheres or MBraun drybox under an atmosphere of purified nitrogen or argon. Diethyl ether, toluene, *n*-pentane, *n*-hexane, and THF were dried and deoxygenated by the method of Grubbs.[5] THF was passed through a MBraun solvent purification system, further dried by stirring with sodium metal and then filtered through alumina before use. Distilled solvents were transferred under vacuum into vacuum-tight vessels before being transferred into a Vacuum Atmospheres drybox. C_6D_6 was purchased from Cambridge Isotopes and was degassed and dried over 4 Å molecular sieves. The 4 Å molecular sieves and Celite were dried in vacuo overnight at a temperature above 200 °C. Compounds **2**,[6,7] HN(*t*-Bu)Ar,[8] and $MoCl_3(THF)_3$[9] were prepared following literature methods. $HMo(CO)_3(Cp)$ (**1**-H, Cp = η^5-C_5H_5) was prepared by reaction of $Mo(CO)_3$(*p*-xylene) and C_5H_6 in THF[10] and purified by high-vacuum sublimation. **1**-D was obtained by stirring a pentane solution of **1**-H over a large excess of D_2O for several hours, separating the organic phase, evaporating it to dryness, and then subliming **1**-D. Analysis by NMR showed it to be ∼95% D and 5% H substituted. PhCN was distilled under reduced pressure before use and stored in a nitrogen-filled drybox. All other compounds were used as received. ^1H and ^{13}C NMR spectra were recorded on Unity 300, Mercury 300, Bruker AVANCE-400, or Varian INOVA-500 spectrometers at room temperature. ^{13}C NMR spectra are proton decoupled. Chemical shifts are reported with respect to internal solvent: 7.16 and 128.38 (t) ppm (C_6D_6) for ^1H and ^{13}C, respectively. FTIR spectra were obtained using a Perkin-Elmer 2000 FTIR/Microscope system that has been described elsewhere.[11] CHN analyses were performed by H. Kolbe Mikroanalytisches Laboratorium (Mülheim, Germany) or Midwest Microlabs LLC (Indianapolis, IL).

Synthesis of $HMo(N[t\text{-}Bu]Ar)_3$ (2-H). A solution of $H_2Sn(n\text{-}Bu)_2$ (1.346 g, 5.80 mmol) or H_2SnPh_2 (0.480 g, 1.74 mmol) in 5 mL of Et_2O was added dropwise to a 50 mL round-bottom flask containing an orange-brown solution of **2** (1.864 g, 2.90 mmol) in 20 mL of Et_2O. The resulting solution turned dark red rapidly and was stirred for 1 h at 20 °C. The solution was filtered through a plug of Celite. Upon removal of all volatile components, a brick-red solid was obtained, extracted into a minimum amount of *n*-pentane, and stored at −35 °C to give 1.718 g (2.75 mmol) of brick-red powder (92% yield).

In addition, **2**-H was synthesized using **1**-H as the H-atom donor. In a scintillation vial, a solution of **1**-H (119 mg, 0.48 mmol) in 2 mL of pentane was added to a solution of **2** (300 mg, 0.48 mmol) in 15 mL of *n*-pentane giving a dark red solution. After it was stirred for 2 h at T = 20 °C, the reaction mixture was filtered. Volatile materials

(1) Mendiratta, A.; Cummins, C. C.; Kryatova, O. P.; Rybak-Akimova, E. V.; McDonough, J. E.; Hoff, C. D. *J. Am. Chem. Soc.* **2006**, *128*, 4881.
(2) Figueroa, J. S.; Cummins, C. C. *J. Am. Chem. Soc.* **2003**, *125*, 4020.
(3) Debad, J. D.; Legzdins, P.; Lumb, S. A.; Batchelor, R. J.; Einstein, F. W. D. *Organometallics* **1995**, *14*, 2543.
(4) (a) Schelter, E. J.; Yang, P.; Scott, B. L.; Da Re, R. E.; Jantunen, K. C.; Martin, R. L.; Hay, P. J.; Morris, D. E.; Kiplinger, J. L. *J. Am. Chem. Soc.* **2007**, *129*, 5139. (b) Schelter, E. J.; Yang, P.; Scott, B. L.; Thompson, J. D.; Martin, R. L.; Hay, P. J.; Morris, D. E.; Kiplinger, J. L. *Inorg. Chem.* **2007**, *46*, 7477. (c) Jantunen, K. C.; Burns, C. J.; Castro-Rodriguez, I.; Da Re, R. E.; Golden, J. T.; Morris, D. E.; Scott, B. L.; Taw, F. L.; Kiplinger, J. L. *Organometallics* **2004**, *23*, 4682.
(5) Pangborn, A. B.; Giardello, M. A.; Grubbs, R. H.; Rosen, R. K.; Timmers, F. *Organometallics* **1996**, *15*, 1518.
(6) Laplaza, C. E.; Johnson, M. J. A.; Peters, J. C.; Odom, A. L.; Kim, E.; Cummins, C. C.; George, G. N.; Pickering, I. J. *J. Am. Chem. Soc.* **1996**, *118*, 8623.
(7) Laplaza, C. E.; Odom, A. L.; Davis, W. M.; Cummins, C. C. *J. Am. Chem. Soc.* **1995**, *117*, 4999.
(8) Tsai, Y. -C.; Stephens, F. H.; Meyer, K.; Mendiratta, A.; Gheorghiu, M. D.; Cummins, C. C. *Organometallics* **2003**, *22*, 2902.
(9) Stoffelbach, F.; Saurenz, D.; Poli, R. *Eur. J. Inorg. Chem.* **2001**, 2699.
(10) Hoff, C. D. *J. Organomet. Chem.* **1985**, *282*, 201.
(11) Ju, T. D.; Capps, K. B.; Roper, G. C.; Hoff, C. D. *Inorg. Chim. Acta* **1998**, *270*, 488.

were removed under reduced pressure, and 235 mg (0.38 mmol, 78% yield) of pure **2**-H was isolated. ^{1}H NMR (400 MHz, T = 20 °C, C_6D_6): δ = 28.13 (s, 27H, C*(CH$_3$)$_3$*), −7.54 (s, 18H, C_6H_3*(CH$_3$)$_2$*), −18.28 (br, s, 6H, *o-ArH*), −26.71 (s, 3H, *p-ArH*) ppm. IR: ν_{Mo-H} = 1860 cm^{-1}, ν_{Mo-D} = 1334 cm^{-1}. μ_{eff} = 3.09 μ_B (Evans' method,[12] C_6D_6, 19.8 °C). Anal. Calcd for $C_{36}H_{55}N_3Mo$: C, 63.17; H, 6.83; N, 4.91. Found: C, 62.97; H, 6.90; N, 4.81.

Synthesis of (Ph(H)C=N)Mo(N[*t*-Bu]Ar)$_3$ (2-NC(H)Ph). A scintillation vial was charged with **2** (200 mg, 0.32 mmol) and 5 mL of *n*-pentane. PhCN (33 mg, 0.32 mmol) was added resulting in a rapid color change to purple. To this solution was added solid **1**-H (79 mg, 0.32 mmol), and the solution was allowed to stir for 40 min. After this time, the solution was dark blue, and copious amounts of red precipitate had formed. The reaction mixture was filtered through Celite, and the volatile components were removed under dynamic vacuum. Recrystallization from Et_2O (−35 °C) furnished **2**-NC(H)Ph as large blue blocks (2 crops, 123 mg, 53% yield). ^{1}H NMR (500 MHz, T = 20 °C, C_6D_6): δ = 1.30 (s, 27H, C*(CH$_3$)$_3$*), 2.18 (s, 18H, C_6H_3*(CH$_3$)$_2$*), 6.55 (d, 2H, *o-PhH*), 6.67 (s, 6H, *o-ArH*), 6.67 (t, 1H, *p-PhH*), 6.69 (s, 3H, *p-ArH*), 7.17 (t, 2H, *m-Ph*), 7.44 (s, 1H, *N* = C*H*) ppm. ^{13}C NMR (75 MHz, T = 20 °C, C_6D_6): δ = 21.31 (C_6H_3*(CH$_3$)$_2$*), 31.27 (C*(CH$_3$)$_3$*), 62.28 (N−*C*(CH$_3$)$_3$), 122.28, 124.42, 127.04, 127.30, 129.03, 135.77, 137.23, 150.27, 156.49 ppm. UV−vis (toluene, 20 °C): λ_{max} = 410, 585 nm. Anal. Calcd for $C_{43}H_{60}N_4Mo$: C, 70.86; H, 8.30; N, 7.69. Found: C, 70.66; H, 8.23; N, 7.31.

Insertion of PhCN into 2-H. Four different tubes with a mixture of **2** and 0.7 equiv of **1**-H were prepared. To three of the samples, 2 equiv of PhCN were added after 3, 20, and 60 min, and then all of them were flame-sealed under vacuum for NMR study. The sample without any added PhCN was used as a control to check the stability of **2**-H over the time period studied. It appeared to be stable; however, after six days, some decomposition occurred based on analysis of the integration data. The initial ^{1}H NMR data run on day 1 showed that the tube that had nitrile added after 3 min had copious amount of **2**-NC(H)Ph and the other two tubes had sequentially more **2**-H and smaller and finally traces of **2**-NC(H)Ph. NMR spectra were taken also after 1, 2, and 5 days. At the end of day 6, conversion of **2**-NC(H)Ph via nitrile insertion was complete. Figure SF1 shows decay of **2**-H over time for the tube in which the benzonitrile was added after 20 min.

The possibility that the insertion may have occurred slowly by a direct process catalyzed by free **2** forming **2**-NC(H)Ph was investigated by comparing the rates of formation of **2**-NC(H)Ph in the presence of excess added **2** to **2**-H. No significant rate enhancement was observed.

Crystallographic Structure Determinations. X-ray diffraction data were collected using a Siemens Platform three-circle diffractometer coupled to a Bruker-AXS Smart Apex CCD detector with graphite-monochromated Mo Kα radiation (λ = 0.71073 Å), performing ϕ- and ω-scans. The structure was solved by direct methods using SHELXS[13] and refined against F^2 on all data by full-matrix least-squares with SHELXL-97.[14] All non-hydrogen atoms were refined anisotropically; all hydrogen atoms were included into the model at their geometrically calculated positions and refined using a riding model except in the case of **2**-H, where the hydride position was located from the electronic density difference map.

Enthalpy of Reaction of 2 and 1-H. In the glovebox, a solution of **2** (0.1545 g, 0.247 mmol) was prepared in 5 mL of freshly distilled toluene and transferred via syringe through a Teflon syringe filter into the calorimeter cell under argon atmosphere. A sample of freshly sublimed **1**-H (0.0242 g, 0.098 mmol) was loaded into the solid sample holder of the calorimeter cell. The cell was sealed, taken from the glovebox, and loaded into a Setaram C-80 calorimeter. After thermal equilibration, approximately two hours, the reaction was initiated and followed to completion at 30 °C. Following the return to baseline, the cell was taken back into the glovebox, and its contents examined by FTIR to confirm conversion of **1**-H to **1**$_2$. A small residual band at 1864 cm^{-1} indicated a trace amount of the proposed intermediate complex (Ar[*t*-Bu]N)$_3$Mo−Mo(CO)$_3$(Cp) (**1**−**2**). A separate calorimetric study of the enthalpy of reaction of **2** and **1**$_2$ was undertaken and indicated that ΔH = −12 ± 2 kcal mol^{-1} for formation of the proposed metal−metal bonded complex. Estimated corrections for the trace amounts of (Ar[*t*-Bu]N)$_3$Mo−Mo(CO)$_3$(Cp) detected in the calorimetric reactions of **2** and **1**-H were below experimental error limits and are not included in the reported average value based on six independent determinations of ΔH = −10.0 ± 0.7 kcal mol^{-1} for the enthalpy of reaction based on solid **1**-H. The enthalpy of solution of **1**-H in toluene is ΔH = 3.1 ± 0.1 kcal mol^{-1} yielding a value with all species in solution of ΔH = −13.1 ± 0.7 kcal mol^{-1}.

Enthalpy of Reaction of 2-NCPh and 1-H. In the glovebox, a solution of **2** (3.7 g, 14.9 mmol) was prepared in 200 mL of toluene. The filtered solution was then taken from the glovebox and transferred under argon atmosphere to an isoperibol calorimeter system with an internal capacity of 300 mL. The calorimeter was thermally equilibrated at 20 °C for a period of 2 h. At that time, 10 mL of freshly distilled benzonitrile was added, and the solution turned into the dark purple color characteristic of **2**-NCPh. Following an equilibration time of about 10 min, the calorimeter was electrically calibrated. Sealed glass ampoules containing 0.1949, 0.1828, and 0.1524 g of **1**-H were broken into the solution. Following that, additional electrical calibrations were performed. It is known that **2**-NCPh forms a dimer slowly in solution under these conditions; however the rapid nature of the reaction and the use of a large excess of **2**-NCPh allowed reasonable instrument performance because any heat evolved during the relatively slow dimerization was absorbed into the baseline for both calorimetric runs, as well as electrical calibrations. The values determined, ΔH = −34.25, −30.22, and −31.77 kcal mol^{-1} yield an average value of the enthalpy of reaction based on solid **1**-H of ΔH = −32.0 ± 2.0 kcal mol^{-1} giving a value with all species in solution of ΔH = −35.1 ± 2.1 kcal mol^{-1} using the enthalpy of solution of **1**-H in toluene (ΔH = 3.1 ± 0.1 kcal mol^{-1}).

Stopped Flow Kinetic Measurements. Toluene solutions of the reagents were prepared in a MBraun glovebox filled with argon and placed in Hamilton gastight syringes. Time-resolved spectra (400−700 nm) were acquired at temperatures from −30 to −10 °C using a Hi-Tech Scientific (Salisbury, Wiltshire, U.K.) SF-43 Multi-Mixing CryoStopped-Flow Instrument in diode array mode. The stopped-flow instrument was equipped with stainless steel plumbing, a 1.00 cm^3 stainless steel mixing cell with sapphire windows, and an anaerobic gas-flushing kit. The instrument was connected to an IBM computer with IS-2 Rapid Kinetic software (Hi-Tech Scientific). The temperature in the mixing cell was maintained to ±0.1 °C, and the mixing time was 2−3 ms. The driving syringe compartment and the cooling bath, filled with heptane (Fisher), were flushed with argon before and during the experiments, using anaerobic kit flush lines. All flow lines of the SF-43 instrument were extensively washed with degassed, anhy-

(12) (a) Evans, D. F. *J. Chem. Soc.* **1959**, 2003. (b) Bottomley, F.; Lin, I. J. B. *J. Chem. Soc., Dalton Trans.* **1981**, 271.
(13) Sheldrick, G. M. *Acta Crystallogr., Sect. A: Found. Crystallogr.* **1990**, *A46*, 467.
(14) Sheldrick, G. M. *SHELXL-97*; University of Göttingen: Göttingen, Germany, 1997.

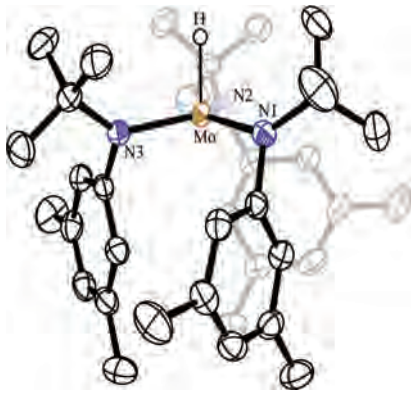

Figure 1. Thermal ellipsoid plot (50% probability) of HMo(N[*t*-Bu]Ar)$_3$. Selected distances (Å) and angles (deg): Mo−H, 1.58(3); Mo−N1, 1.967(2); Mo−N2, 1.960(2); Mo−N3, 1.957(2); N1−Mo−N2, 119.46(8); N2−Mo−N3, 116.75(8); N3−Mo−N1, 120.02(8); H−Mo−N1, 98(1); H−Mo−N2, 96(1); H−Mo−N3, 95(1).

drous toluene before charging the driving syringes with reactant solutions. The reactions were studied by rapid scanning spectrophotometry under pseudo-first-order conditions (0.3 mM for **2** and premixed solution of 50 mM for PhCN and 4 mM for **1**-H or **1**-D). The rate dependence on [XMo(CO)$_3$(C$_5$H$_5$)] (X = H, D) was studied at −30 °C varying [XMo(CO)$_3$(C$_5$H$_5$)] from a 1- to 15-fold excess, and the reaction order in XMo(CO)$_3$(C$_5$H$_5$) was established. All of the experiments were performed in a single-mixing mode of the instrument, with a 1:1 (v/v) mixing ratio. The reactions were monitored for three to five half-lives. A series of three to six measurements at each temperature gave an acceptable standard deviation (within 10%). Data analysis was performed with IS-2 Rapid Kinetic software from Hi-Tech Scientific or Spectfit/32 Global Analysis System software from Biologic. Single-exponential kinetic profiles were observed in all experiments.

Results and Discussion

Preparation and X-Ray Structure of 2-H. Preparation of **2**-H was first achieved with organotin dihydrides[15] as shown in reaction 2

$$2\mathrm{Mo(N[}t\text{-Bu]Ar)}_3 + \mathrm{H_2SnR_2} \xrightarrow[(\mathrm{R} = n\text{-Bu},\ \mathrm{Ph})]{} 2\mathrm{HMo(N[}t\text{-Bu]Ar)}_3 + 1/n(\mathrm{R_2Sn})_n \quad (2)$$

It was observed that addition of 2 equiv of H$_2$Sn(*n*-Bu)$_2$ was necessary to achieve complete formation of the paramagnetic brick-red Mo(IV) complex, **2**-H, whereas only 0.6 equiv of H$_2$SnPh$_2$ were needed. This is consistent with the better H-donor ability of H$_2$SnPh$_2$ over H$_2$Sn(*n*-Bu)$_2$.[16] Attempts to directly hydrogenate **2** under 1000 psi H$_2$ at T = 20 °C show slow reaction with ≤4% conversion to **2**-H in 16 h despite the expected thermochemical favorability (vide infra).

The solid-state structure of **2**-H is shown in Figure 1. It clearly shows a trigonal-monopyramidal complex with C_3 symmetry.[17] The geometry of the Mo−N$_3$ unit is almost planar with the sum of N−Mo−N angles = 356.23°. Similarly, the sum of the same angles in complex **2**[7] and ClMo(N[*t*-Bu]Ar)$_3$[18] are 357.7(3)° and 350(1)° respectively. The small deviation from planarity at Mo in **2**-H can be attributed to the lack of π interaction between molybdenum and the hydride ligand. The sum of the three N−Mo−N angles in ClMo(N[*t*-Bu]Ar)$_3$ is slightly smaller than that observed in **2**-H because of the presence of π-bonding between molybdenum and the chloride ligand, as well as the relative bulk of the Cl atom. The three 3,5-C$_6$H$_3$Me$_2$ substituents are on one side of the trigonal plane and the three *t*-Bu groups on the other. The experimentally determined Mo−H interatomic distance of 1.58(3) Å is similar to that reported for the W−H bond (between 1.57 and 1.59 Å) in the compound [(Me$_3$SiCH$_2$CH$_2$N)$_3$N]WH.[19] However, since the hydride position was located from the electron density difference map, we do not expect this value to be accurate. Several neutron diffraction studies of molybdenum hydrides have been reported,[20−23] giving values for the Mo−H bond of 1.69,[20] 1.685,[21] 1.716,[22] and 1.789 (average)[23] Å for the complexes Mo(H)(η^2-Me$_2$C=NAr)(N[*i*-Pr]Ar)$_2$, H$_2$Mo(η^5-C$_5$H$_5$)$_2$, H$_3$Mo(η^5-1,2,4-C$_5$H$_2$-(*t*-Bu)$_3$)-(PMe$_3$)$_2$, and HMo(CO)$_3$(η^5-C$_5$Me$_5$), respectively. A similar underestimated Mo−H bond length of 1.58 Å was obtained by X-ray diffraction by Poli and co-workers.[22]

The Mo−H and Mo−D (which was prepared using D$_2$SnR$_2$) stretching frequencies were located at 1860 and 1334 cm^{-1} for Mo−H and Mo−D, respectively, in approximate agreement with harmonic oscillator predictions. The magnetic susceptibility of complex **2**-H, determined using Evans' method,[12] was found to be $\mu_{\mathrm{eff}} = 3.09\ \mu_{\mathrm{B}}$, close to the spin-only value for a d^2 complex (2.83 μ_{B}). This magnetic property can be explained in terms of the electronic structure of **2**-H. Since no π-interaction exists between the hydride ligand and molybdenum, the half-occupied π orbitals (d$_{xz}$ and d$_{yz}$, taking the Mo−H vector as the z axis in the C_3 point group) remain degenerate in the complex. Hence, the C_3 symmetric compound is expected to remain paramagnetic with two unpaired electrons in the degenerate d$_{xz}$ and d$_{yz}$ orbitals.

H/D Exchange in Reaction of H$_2$ and DMo(N[*t*-Bu]-Ar)$_3$. The deuterated isotopomer, **2**-H, reacts with H$_2$ (4 atm) at T = 20 °C to produce the hydride complex, which was identified by IR spectroscopy. A reasonable mechanism for this reaction is proposed in eq 3

$$\begin{array}{ccccc} \mathrm{DMo(N[}t\text{-Bu]Ar)}_3 + \mathrm{H_2} & & \mathrm{DH_2Mo(N[}t\text{-Bu]Ar)}_3 & & \mathrm{HMo(N[}t\text{-Bu]Ar)}_3 + \mathrm{HD} \\ \rightleftharpoons & \rightleftharpoons & & \rightleftharpoons & \\ \mathrm{D(H_2)Mo(N[}t\text{-Bu]Ar)}_3 & & & \mathrm{(HD)(H)Mo(N[}t\text{-Bu]Ar)}_3 & \end{array} \quad (3)$$

Schrock and co-workers prepared the W(VI) trihydride complex, [(Me$_3$SiCH$_2$CH$_2$N)$_3$N]WH$_3$, by treating [(Me$_3$Si-CH$_2$CH$_2$N)$_3$N]WH with H$_2$.[19] Despite the failure to spectroscopically detect H$_3$Mo(N[*t*-Bu]Ar)$_3$, this provides reasonable precedent for a trihydride intermediate being formed, albeit in low concentrations, as part of the H/D exchange mechanism. While a trihydride complex such as that proven in ref 19 seems to be the most logical intermediate in this

(15) Tsai, Y.-C. PhD thesis, Massachusetts Institute of Technology, Cambridge, MA, 2002.
(16) Kuivila, H. G. *Synthesis* **1970**, 499.
(17) Cummins, C. C.; Lee, J.; Schrock, R. R.; Davis, W. D. *Angew. Chem., Int. Ed.* **1992**, *31*, 1501.

reaction sequence, other mechanisms (such as σ-bond metathesis)[24] cannot be ruled out.

Preparation and X-Ray Structure of 2-NC(H)Ph. Compound **2**-NCPh has been shown to behave as a carbon-based radical.[1,8,25] Because hydrogen atom abstraction is a typical reaction of carbon-based radicals,[26] it was decided to examine the reactivity of **2**-NCPh with a variety of H-atom donors as shown in reaction 4.

$$\mathrm{PhCN{-}Mo(N[}t\text{-Bu]Ar)_3} \xrightarrow[\mathrm{Et_2O}]{[\mathrm{H}]} \mathrm{Ph(H)CN{-}Mo(N[}t\text{-Bu]Ar)_3}$$
$$[\mathrm{H}] = \mathrm{HMo(CO)_3(C_5H_5)}, \mathrm{H_2Sn(}n\text{-Bu)_2}$$
$$\text{no reaction with } \mathrm{HSn(}n\text{-Bu)_3} \quad (4)$$

When a freshly prepared, purple, pentane solution of **2**-NCPh is treated with 1 equiv of crystalline **1**-H,[27] a color change to deep blue, along with precipitation of a red solid is observed over a period of 5 min. Removal of the red solid (**1**$_2$), followed by crystallization from Et_2O, resulted in the isolation of **2**-NC(H)Ph as large blue blocks in 53% yield. Compound **2**-NC(H)Ph is diamagnetic and exhibits a ^{1}H NMR resonance at $\delta = 7.41$ ppm attributed to the ketimide proton.

The solid-state structure of **2**-NC(H)Ph is shown in Figure 2. Of note is the short Mo−N(4) distance of 1.7896(12) Å as compared to the average Mo−amide distance of 1.973 Å. This contraction is likely a consequence of the hybridization change upon going from an amide to a ketimide nitrogen, as well as both the π-acceptor and π-donor character of the ketimide ligand. The ability of the N−C π^* orbital to act as a π acceptor is facilitated by the nearly linear (166.84(11)°) Mo−N−C angle. A relevant structural comparison is to the parent ketimide complex $(H_2C{=}N)Mo(N[t\text{-Bu}]Ar)_3$ prepared by deprotonation of the cationic methylimido complex.[28] Compared to **2**-NC(H)Ph, $(H_2C{=}N)Mo(N[t\text{-Bu}]Ar)_3$ features similar Mo−N and N−C distances (1.777(4) and 1.300(7) Å, respectively), although the Mo−N−C unit is considerably closer to linearity (Mo−N−C = 178.04(4)°). In addition, the nitrosyl complex $(O{=}N)Mo(N[Ad]Ar)_3$ displays an Mo−N−O angle of 179.7°.[29] One possible rationalization for the slight deviation from linearity in **2**-NC(H)Ph is that

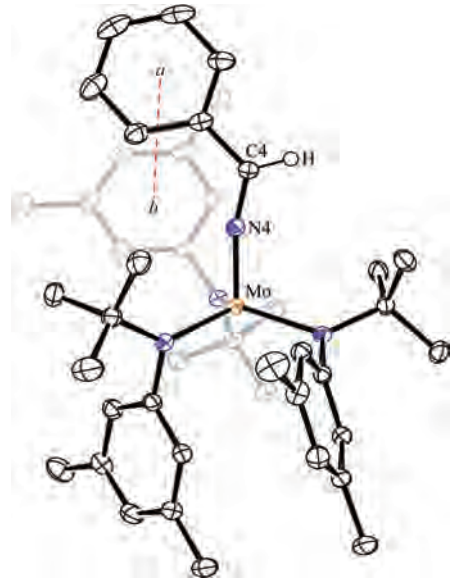

Figure 2. Solid-state structure (50% ellipsoids) of Ph(H)CN-Mo(N[*t*-Bu]Ar)$_3$ (**2**-NC(H)Ph). Selected bond distances (Å): Mo−N$_{amide}$, 1.973 (average); Mo−N4, 1.7896(12); N4−C4, 1.3055(17); distance between centroids (*a*−*b*), 4.113. Selected bond angles (deg): Mo−N4−C4, 166.84(11).

there may be a π-stacking interaction between the phenyl residue on the ketimide and the aryl substituent on one of the amido groups bound to molybdenum. The aromatic rings are neither parallel to each other nor in an eclipsed sandwich configuration but are displaced and tilted to form an angle of 19.94°. The distance between the centroids is 4.113 Å, and the shortest distance between the rings is 3.267 Å. This compares to the observation that in the solid crystalline form many aromatic molecules form stacks with displaced rings in approximately parallel molecular planes separated by 3.3−3.6 Å[30] and in the case of tilted compounds form angles between 15 and 40° with a distance of 4.4−4.7 Å between centroids.[31] This interaction results in reversal of the configuration of one of the anilides, a situation that has been previously noticed in $(Ph(PhX)C{=}N)Mo(N[t\text{-Bu}]Ar)_3$[25] (X = S, Se) and $((H_3C)_3SiO(Ph)C{=}N)Mo(N[t\text{-Bu}]Ar)_3$[32] where the anilide ligands also adopt an up−down-sideways conformation. However, in cases where this interaction is not possible, such as in the parent ketimide $(H_2C{=}N)Mo(N[t\text{-Bu}]Ar)_3$[28] or $((H_3C)_3SiO(t\text{-Bu})CN)Mo(N[t\text{-Bu}]Ar)_3$,[33] the conformation of the $Mo(N[t\text{-Bu}]Ar)_3$ moiety is one of near C_3 symmetry, in agreement with this proposition.

Compound **2**-NC(H)Ph can also be prepared by reaction of **2**-NCPh with 0.5 equiv $H_2Sn(n\text{-Bu})_2$. While the reaction appears to be quantitative by ^{1}H NMR, the presence of the Sn side product hinders isolation, rendering the former method more attractive for synthetic purposes. Interestingly, **2**-NCPh shows no reaction with $HSn(n\text{-Bu})_3$, consistent with the previous observation that $HSn(n\text{-Bu})_3$ is a less active H-atom donor than $H_2Sn(n\text{-Bu})_2$.[16]

(18) Fürstner, A.; Mathes, C.; Lehmann, C. W. *J. Am. Chem. Soc.* **1999**, *121*, 9453.
(19) Dobbs, A. A.; Schrock, R. R.; Davis, W. M. *Inorg. Chim. Acta* **1997**, *263*, 171.
(20) Tsai, Y. -C.; Johnson, M. J. A.; Mindiola, D. J.; Cummins, C. C. *J. Am. Chem. Soc.* **1999**, *121*, 10426.
(21) Schultz, A. J.; Stearley, K. L.; Williams, J. M.; Mink, R.; Stucky, G. D. *Inorg. Chem.* **1977**, *16*, 3303.
(22) Baya, M.; Houghton, J.; Daran, J. -C.; Poli, R.; Male, L.; Albinati, A.; Gutman, M. *Chem.—Eur. J.* **2007**, *13*, 5347.
(23) Brammer, L.; Zhao, D.; Bullock, R. M.; McMullan, R. K. *Inorg. Chem.* **1993**, *32*, 4819.
(24) Thompson, M. E.; Baxter, S. M.; Ray Bulls, A.; Burger, B. J.; Nolan, M. C.; Santarsiero, B. D.; Schaefer, W. P.; Bercaw, J. E. *J. Am. Chem. Soc.* **1987**, *109*, 203.
(25) Mendiratta, A.; Cummins, C. C.; Kryatova, O. P.; Rybak-Akimova, E. V.; McDonough, J. E.; Hoff, C. D. *Inorg. Chem.* **2003**, *42*, 8621.
(26) *Free Radicals*, Vol. II; Kochi, J. K., Ed.; Wiley: New York, 1973.
(27) (a) Landrum, J. T.; Hoff, C. D. *J. Organomet. Chem.* **1985**, *282*, 215. (b) Amer, S.; Kramer, G.; Poe, A. *J. Organomet. Chem.* **1981**, *220*, 75.
(28) Sceats, E. L.; Figueroa, J. S.; Cummins, C. C.; Loening, N. M.; Van der Wel, P.; Griffin, R. G. *Polyhedron* **2004**, *23*, 2751.
(29) Cummins, C. C. *Prog. Inorg. Chem.* **1998**, *47*, 768.
(30) Dahl, T. *Acta Chem. Scand.* **1994**, *48*, 95.
(31) Sony, S. M. M.; Ponnuswamy, M. N. *Cryst. Growth Des.* **2006**, *6*, 737.
(32) Curley, J. J.; Sceats, E. L.; Cummins, C. C. *J. Am. Chem. Soc.* **2006**, *128*, 14036.
(33) Curley, J. J.; Cummins, C. C. Unpublished results.

Benzonitrile Insertion into 2-H. On the basis of estimates of bond strengths (vide infra), it was predicted that benzonitrile insertion into complex **2**-H should be thermodynamically favorable. Reaction 5 was observed to occur; however it was extremely slow even in the presence of 20 equiv of benzonitrile. The reaction requires about one week to go to completion at $T = 20$ °C. NMR data supporting this conclusion are shown in Supporting Information Figure SF1.

$$HMo(N[t\text{-}Bu]Ar)_3 + PhCN \rightarrow (Ph(H)C{=}N)Mo(N[t\text{-}Bu]Ar)_3 \quad (5)$$

The slow nature of this reaction led us to investigate its catalysis. Provided that H atom transfer in reaction 7 is rapid, addition of free **2** to **2**-H would be expected to increase the rate of reaction 5 by the combined sequence of reactions 6 and 7

$$Mo(N[t\text{-}Bu]Ar)_3 + PhCN \rightleftharpoons (PhCN)Mo(N[t\text{-}Bu]Ar)_3 \quad (6)$$

$$\begin{array}{ccc} (PhCN)Mo(N[t\text{-}Bu]Ar)_3 & & (Ph(H)C{=}N)Mo(N[t\text{-}Bu]Ar)_3 \\ + & \rightarrow & + \\ HMo(N[t\text{-}Bu]Ar)_3 & & Mo(N[t\text{-}Bu]Ar)_3 \end{array} \quad (7)$$

Contrary to our expectations, no significant rate enhancement was observed for nitrile insertion into the H−Mo bond in the presence of free added **2**. Instead, the previously reported slow dimerization of **2**-NCPh was observed.[8]

The most plausible mechanism for the slow insertion of nitrile into the H−Mo bond involves coordination of nitrile at **2**-H in a transition state geometry similar to that shown in Figure 3. This transition state configuration resembles that proposed for the thermodynamically favored β-X elimination step in the reactions shown in Scheme 1. Additional support for this is gleaned from the fact that H_2 undergoes H/D exchange with $DMo(N[t\text{-}Bu]Ar)_3$ (vide supra). This implies some ability on the part of **2**-H to coordinate added ligands. The fact that there is a spin change in going from a ground-state triplet in **2**-H to a singlet in **2**-NC(H)Ph would be expected to further increase the activation energy[34] for this thermodynamically favorable reaction.

Thermochemistry of Reaction of 1-H and 2. In the presence of **1**-H, conversion of **2** to **2**-H occurs quantitatively in toluene solution at 30 °C according to reaction 8

$$\begin{array}{ccc} Mo(N[t\text{-}Bu]Ar)_3 & & HMo(N[t\text{-}Bu]Ar)_3 \\ + & \rightarrow & + \\ HMo(CO)_3(Cp) & & 1/2[Mo(CO)_3(Cp)]_2 \end{array} \quad (8)$$

As discussed in a later section, this reaction involves generation and disappearance of small amounts of complex **1**−**2**, but the enthalpy of reaction at 30 °C with all species in toluene solution was determined as $\Delta H = -13.1 \pm 0.7$ kcal mol^{-1}. The enthalpy of hydrogenation of $\mathbf{1}_2$ as shown in reaction 9 has been previously reported as +6.3 kcal mol^{-1}:[27a,35]

$$[Mo(CO)_3(Cp)]_2 + H_2 \rightarrow 2HMo(CO)_3(Cp) \quad (9)$$

The addition of twice reaction 8 to reaction 9 yields directly a computed enthalpy of hydrogenation for reaction 10 of $\Delta H = -19.9 \pm 1.4$ kcal mol^{-1}.

$$2Mo(N[t\text{-}Bu]Ar)_3 + H_2 \rightarrow 2HMo(N[t\text{-}Bu]Ar)_3 \quad (10)$$

These data yield an estimate for the Mo−H bond strength in **2**-H of 62 kcal mol^{-1}. The Mo−H bond dissociation energy in **1**-H has been estimated previously using calorimetric measurements (BDE = 66 kcal mol^{-1})[10,27a] and by employing a combination of the pK_a with the experimentally determined oxidation potential of $\mathbf{1}^-$ (BDE = 70 kcal mol^{-1}).[36] The Mo−H bond strengths in **2**-H and **1**-H are surprising because they indicate a stronger Mo−H bond in **1**-H. This is in contrast to other Mo−X BDE values in these systems where the **2** molecule generally forms stronger Mo−X bonds. For example, the $(PhS)Mo(N[t\text{-}Bu]Ar)_3$ Mo−S bond strength[37] of 55 kcal mol^{-1} compares to data for the $(PhS)Mo(CO)_3(C_5H_5)$ bond strength[38] of 38 kcal mol^{-1}. Because the spontaneous direction of reaction 8 produces a complex with a weaker H−Mo bond, it is formation of the metal−metal bond in $\mathbf{1}_2$ that provides the thermochemical driving force. As is well known, because of steric factors, **2** does not form the expected metal−metal triple bond,[39] which would be anticipated to significantly alter the thermochemical profile of the hydrogenation reaction in eq 10.

Thermochemistry of Reaction of 1-H and 2-NCPh. As discussed in a later section, reaction 11 is rapid and quantitative even at low temperatures.

$$\begin{array}{ccc} (PhCN)Mo(N[t\text{-}Bu]Ar)_3 & & (Ph(H)C{=}N)Mo(N[t\text{-}Bu]Ar)_3 \\ + & \rightarrow & + \\ HMo(CO)_3(Cp) & & 1/2[Mo(CO)_3(Cp)]_2 \end{array} \quad (11)$$

The enthalpy of reaction 11 with all species in toluene solution at 20 °C was determined as $\Delta H = -35.1 \pm 2.1$ kcal mol^{-1}. The addition of twice the enthalpy of reaction 11 to that of reaction 9 yields directly a value of $\Delta H = -76.5$ kcal mol^{-1} for reaction 12

$$2(PhCN)Mo(N[t\text{-}Bu]Ar)_3 + H_2 \rightarrow 2(Ph(H)C{=}N)Mo(N[t\text{-}Bu]Ar) \quad (12)$$

These data in combination with the BDE of H_2 lead to an estimate of 90 kcal mol^{-1} for the C−H bond dissociation energy in **2**-NC(H)Ph. The C−H bond strength in the [Ph(H)C═N] radical has not been reported, but data for the $H_2C{=}N$ radical indicate a C−H bond strength of 33 ± 6 kcal mol^{-1}.[40] The large difference in C−H bond strength for the complex **2**-NC(H)Ph is attributed to the strength of the Mo−N bond. This is illustrated in the thermochemical cycle in reaction eq 13.

These data lead to the estimate that the bond between **2** and (Ph(H)C═N·) is on the order of 71 ± 8 kcal mol^{-1}.

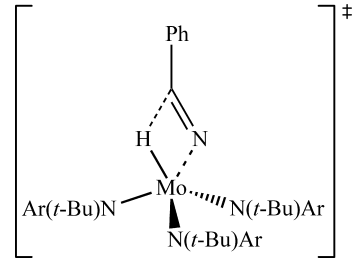

Figure 3. Proposed transition state for insertion of benzonitrile into $HMo(N[t\text{-}Bu]Ar)_3$.

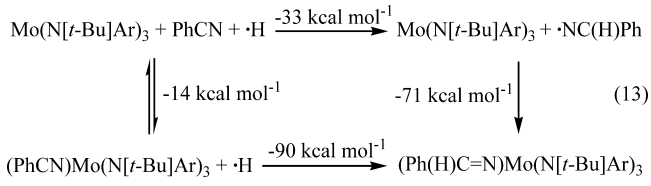

(13)

The enthalpy of binding of the isoelectronic formal three electron donor ligand ·NO to **2** was measured experimentally as −82.5 kcal mol^{-1}.[41] It seems most reasonable to view these complexes as approaching reduced Mo(II) complexes of the cationic NO^+ and $[Ph(H)C{=}N]^+$ ligands and as having an approximate Mo═N═X (X = O, C(H)Ph) formulation.[42] Despite the relatively large error in the estimate in reaction 13, it appears that the metal−ligand bond strength decreases in going from a nitrosyl to a ketimide for binding to **2**.

Combination of the data for the enthalpy of binding of nitrile determined from K_{eq} studies (ca. −14 kcal mol^{-1})[43] and the enthalpy of reactions 8 and 11 measured in this work leads to a calculated exothermic insertion of benzonitrile of −36 kcal mol^{-1} as shown in the thermochemical cycle in Figure 4. Compared to insertion into the Mo−X bond [X = OC(O)Ph (+2.4 kcal mol^{-1}), SePh (−5.8 kcal mol^{-1}), SPh (−10 kcal mol^{-1})], the reverse of the nitrile elimination step shown in Scheme 1), and considering the unfavorable entropy associated with nitrile insertion, it is only for X = H (−36 kcal mol^{-1}) that insertion is predicted to be thermodynamically favored at room temperature and above. As discussed previously, this reaction was observed to occur, albeit slowly over a period of days. In terms of how changing X influences the thermochemistry, it is clear that for X = H, the relatively weak Mo−H bond compared to the strong C−H bond formed would serve to favor this reaction.

Kinetic Study of Reaction of 1-H with 2-NCPh. In contrast to the relatively slow reaction of **1**-H with **2** (vide infra), reaction of **1**-H with **2**-NCPh was found to be too rapid to study by conventional kinetic methods. Stopped flow kinetic methods were used to study the rate of reaction 11 in toluene solution over the temperature range of −10 to −30 °C. The reaction was studied by combination of a mixture of **1**-H and a large excess of PhCN and a solution of **2**. Typical spectral changes observed are shown in Figure 5.

Under the conditions used, the reaction of **2** with excess PhCN to form **2**-NCPh was too fast to be observed. The good fit to kinetic data (Figure 6) and presence of a clean isosbestic point at ∼550 nm (Figure 5) argue for a clean reaction process which was found to be first order in both **1**-H and the in situ generated **2**-NCPh (Figure SF2). In contrast to the slow reaction of **1**-H and **2**, in which the

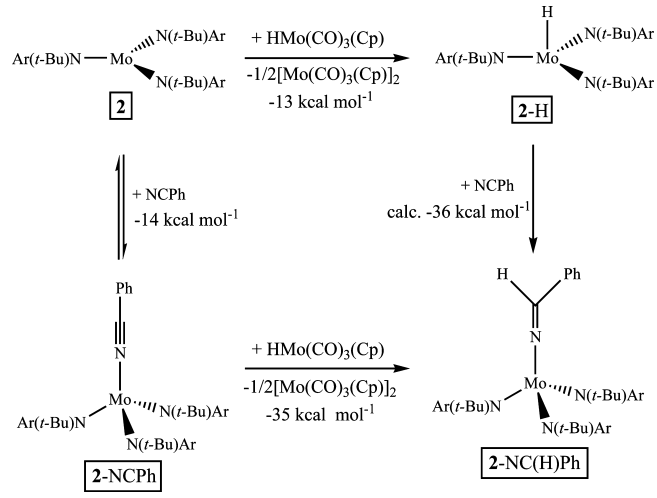

Figure 4. Thermochemical cycle for insertion of benzonitrile.

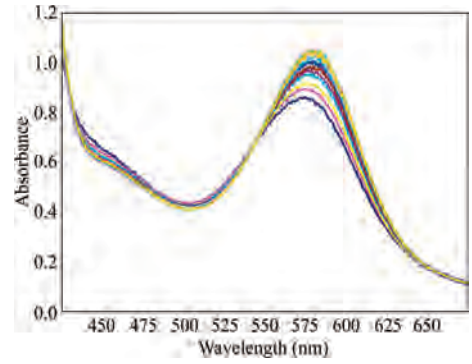

Figure 5. Spectral changes observed at −25 °C upon mixing **2** (0.3 mM) with a premixed solution of PhCN (50 mM) and **1**-H (0.3 mM), time scale = 95 s. The concentrations are given before mixing in the stopped flow cell. The UV−vis spectra of all the compounds involved in the reaction are shown in Supporting Information Figure SF3.

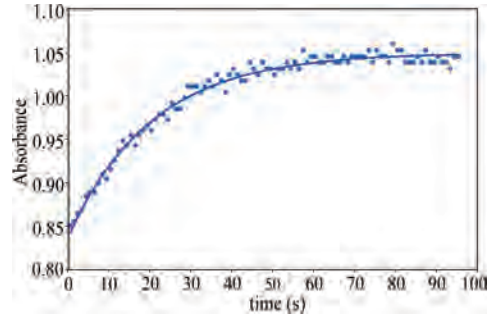

Figure 6. Cross section of the absorbance changes at 580 nm as a function of time for the reaction: **2**-NCPh + **1**-H (T = −25 °C).

(34) Poli, R. *Acc. Chem. Res.* **1997**, *30*, 494.
(35) Nolan, S. P.; Lopez de la Vega, R.; Mukerjee, S. L.; Gonzalez, A. A.; Zhang, K.; Hoff, C. D. *Polyhedron* **1988**, *7*, 1491.
(36) Tilset, M.; Parker, V. D. *J. Am. Chem. Soc.* **1989**, *111*, 6711. (b) Tilset, M.; Parker, V. D. *J. Am. Chem. Soc.* **1990**, *112*, 2843.
(37) McDonough, J. E.; Weir, J. J.; Sukcharoenphon, K.; Hoff, C. D.; Kryatova, O. P.; Rybak-Akimova, E. V.; Scott, B.; Kubas, G. J.; Stephens, F. H.; Mendiratta, A.; Cummins, C. C. *J. Am. Chem. Soc.* **2006**, *128*, 10295.
(38) Mukerjee, S. L.; Gonzalez, A. A.; Nolan, S. P.; Ju, T. D.; Lang, R. F.; Hoff, C. D. *Inorg. Chim. Acta* **1995**, *240*, 175.
(39) *Multiple Bonds between Metal Atoms*, 3rd ed.; Cotton, F. A., Murillo, C. A., Walton, R. A., Eds.; Springer: Berlin, 2005.
(40) (a) Estimate made based on a revised estimate of the enthalpy of formation of H_2CN (ref 40b) based on experimental data (ref 40c), as well as enthalpies of formation for H and HCN taken from NIST webbook. (b) Nesbitt, F. L.; Marston, G.; Stief, L. J.; Wickramaaratchi, W.; Tao, R. B.; Klemm, *J. Phys. Chem.* **1991**, *95*, 7613. (c) Cowles, D. C.; Travers, M. J.; Frueh, J. L.; Ellison, G. B. *J. Chem. Phys.* **1991**, *94*, 3517.
(41) Johnson, A. R.; Baraldo, L. M.; Cherry, J. P. F.; Tsai, Y. C.; Cummins, C. C.; Kryatov, S. V.; Rybak-Akimova, E. V.; Capps, K. B.; Hoff, C. D.; Haar, C. M.; Nolan, S. P. *J. Am. Chem. Soc.* **2001**, *123*, 7271.
(42) Landry, V. K.; Pang, K.; Quan, S. M.; Parkin, G. *Dalton Trans.* **2007**, 820.
(43) Kryatova, O. P.; Rybak-Akimova, E. V.; Mendiratta, A.; Tsai, Y. C.; Cummins, C. C.; McDonough, J. E.; Hoff, C. D. Manuscript in preparation.

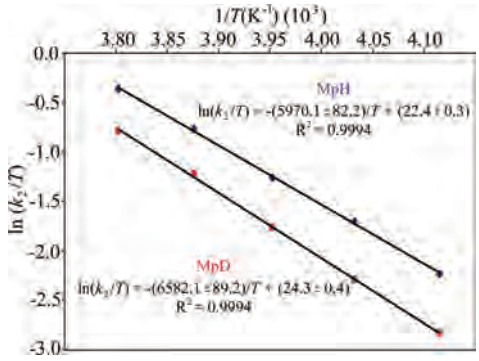

Figure 7. Eyring plot of (Ph(X)C═N)Mo(N[*t*-Bu]Ar)$_3$ formation (X = H, D).

Table 1. Activation Parameters for Reaction of (PhCN)Mo(N[*t*-Bu]Ar)$_3$ with Substrate and BDE of Bond Broken

substrate	$\Delta H^{\ddagger}$ (kcal mol^{-1})	$\Delta S^{\ddagger}$ (cal mol^{-1} K^{-1})	BDE (kcal mol^{-1})
BzOOBz	2.0	−31	19
PhTeTePh	3.7	−29	33
PhSSPh	7.5	−26	46
HMo(CO)$_3$(Cp)	11.9	−2.7	66,[10,27a] 70[36]

complex **1**−**2** was observed, no bands attributable to a significant concentration of an intermediate complex were found for reaction 11 in either UV−vis or FTIR spectra.

Kinetic parameters were determined by monitoring the spectral changes in the 400−700 nm range under pseudo-first-order conditions (excess of **1**-H or **1**-D), yielding essentially wavelength-independent rate constants. Figure 6 shows a typical cross section of the absorbance changes at 580 nm as a function of time for the reaction studied; an excellent fit to a single-exponential rate law was obtained.

Because of the low stability of dilute solutions of **2**, different batches of freshly prepared samples of **2** were used, and reproducible data for this highly air-sensitive reaction system could be obtained. A complete list of all individual data obtained for k_{obs} as a function of temperature for reaction 11 is collected in Supporting Information Tables ST1 (**1**-H) and ST2 (**1**-D).

In contrast to studies of reaction 8 (vide infra), reaction 11 was found to show a normal kinetic isotope effect with $k_H/k_D \approx 1.6$ with slight variation as a function of temperature. A kinetic isotope effect for **1**-H/**1**-D of 3.38 has been calculated by semiclassical theory.[44] However, maximum isotope effects are expected for symmetric linear transition states, and they are generally lower when steric constraints prevent linearity[45] such as in our current case. A kinetic isotope effect of 1.8, similar to that measured here, has been determined for the H/D atom transfer from HW(CO)$_3$(Cp)/DW(CO)$_3$(Cp) to 4-phenyl-3-penten-1-yl radical,[46] and the same result was obtained for the H$^-$/D$^-$ transfer from HMo(CO)$_3$(Cp)/DMo(CO)$_3$(Cp) to Ph$_3$C$^+$.[47] The slower rate of reaction for **1**-D indicates that cleavage of the (H/D)−Mo bond is important in the transition state. Eyring plots for both **1**-H and **1**-D are shown in Figure 7, from which the derived activation parameters $\Delta H^{\ddagger} = 11.9 \pm 0.4$ kcal mol^{-1}, $\Delta S^{\ddagger} = -2.7 \pm 1.2$ cal K^{-1} mol^{-1} and $\Delta H^{\ddagger} = 13.1 \pm 0.4$ kcal mol^{-1}, $\Delta S^{\ddagger} = 1.1 \pm 1.6$ cal K^{-1} mol^{-1} for **1**-H and **1**-D, respectively, were obtained. The uncertainties assigned to the $\Delta H^{\ddagger}$ and $\Delta S^{\ddagger}$ values were twice the calculated errors in the slope and intercept of the Eyring plot.

The activation parameters obtained in this work can be directly compared with those obtained previously for the reaction of **2**-NCPh with other reagents[1,25,43] (Table 1).

There is a correlation between $\Delta H^{\ddagger}$ and the strength of the bond broken. Surprisingly for a bimolecular reaction, the apparent activation entropy calculated from the Eyring plot for reaction 11 is very small. The rates and activation parameters for reaction of **1**-H with different organic radicals (reaction 14) have been previously reported by the Franz[48] and Norton[49] groups.

$$\cdot R + HMo(CO)_3(Cp) \rightarrow RH + \cdot Mo(CO)_3(Cp) \quad (14)$$

For R = hex-5-enyl, Franz and co-workers found $k = 4.2 \times 10^8$ M^{-1} s^{-1} at $T = 298$ K, $\Delta H^{\ddagger} = 0.47$ kcal mol^{-1}, and $\Delta S^{\ddagger} = -17.5$ cal mol^{-1} K^{-1}, and for R = Ph$_3$C·, Norton et al. determined $k = 514$ M^{-1} s^{-1} at $T = 298$ K, $\Delta H^{\ddagger} = 5.76$ kcal mol^{-1}, and $\Delta S^{\ddagger} = -26.8$ cal mol^{-1} K^{-1}. Interaction of a free organic radical with the molybdenum hydride has a low enthalpy of activation and, even for the relatively sterically unencumbered hex-5-enyl radical, a significant negative entropy of activation.

The higher activation enthalpy and near-zero activation entropy observed in reactivity of the bound nitrile radical in **2**-NCPh may be rationalized in terms of a multistep process, such as a two-step process shown in reaction eq 15.

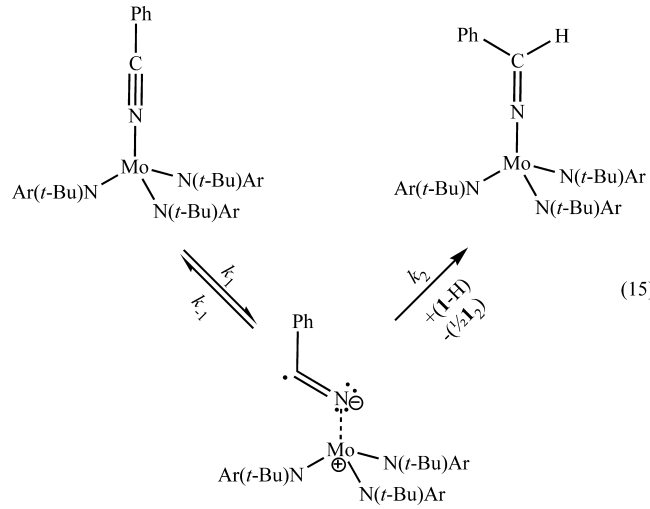

(15)

The first step may involve a pre-equilibrium intramolecular rearrangement of **2**-NCPh leading to a more reactive form of the nitrile complex, in which there is some "loosening" of the molybdenum to nitrile bond. This may be necessary to break, in the second step, the relatively strong H−Mo bond of **1**-H. The higher than expected enthalpy of activation and less negative entropy of activation could result from the fact that the derived

(44) Bullock, R. M. In *Transition Metal Hydrides*; Dedieu, A., Ed.; VCH: New York, 1992; Chapter 8.

activation parameters correspond to the sum of the activation parameters for the pre-equilibrium (k_1/k_{-1}) and H-atom transfer (k_2) steps.

An alternative mechanism to that shown in reaction 15 would involve proton coupled electron transfer[50] as shown in eq 16.

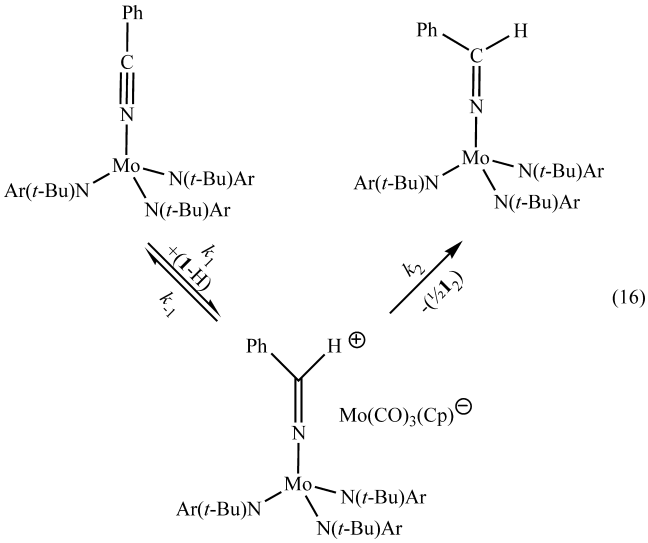

(16)

The first step would involve initial H^+ transfer from **1**-H to **2**-NCPh, followed by electron transfer to ultimately yield products. The normal kinetic isotope effect found would appear to argue against rate-determining electron transfer but does not rule out a proton-coupled electron transfer pathway. Work by Mayer,[51] Abu-Omar,[52] and Bullock[53] has shown that, in some cases, small changes in reactants and conditions can cause a shift in mechanism. It is clear from the data in Table 1 that there is a dramatic difference in the reactivity of **1**-H with **2**-NCPh compared to the other reagents. Additional work aimed at discerning if reaction occurs by direct H atom transfer as shown in eq 15 or proton-mediated electron transfer as shown in eq 16 is planned.

Kinetic Studies of reaction of 1-H with 2. Qualitative spectroscopic studies of the reaction of **1**-H and **2** were investigated by FTIR spectroscopy and gave evidence for buildup and decay of an intermediate complex proposed to be **1**−**2** (Figure 8). The concentration of the intermediate complex was found to increase with increasing [**2**]. The intermediate showed an identical infrared spectroscopic signature to that observed in reaction 17 between $\mathbf{1}_2$ and **2** as shown in Figure 9. Reactions performed at different $\mathbf{2}/\mathbf{1}_2$ ratios showed similar behavior with **1**−**2** formation favored as this ratio increased.

$$\begin{array}{l} \mathrm{Mo(N[}t\text{-Bu]Ar)_3} \\ \quad + \qquad\qquad \rightleftharpoons \mathrm{(Ar[}t\text{-Bu]N)_3Mo\text{-}Mo(CO)_3(Cp)} \\ \mathrm{1/2[Mo(CO)_3(Cp)]_2} \end{array} \tag{17}$$

All attempts to isolate crystalline **1**−**2** failed because it was found to be stable only in the presence of a large excess of **2**. Its formulation is based on spectroscopic evidence. Despite steric crowding around the Mo atom in **2**, precedent for formation of metal−metal-bonded complexes of the type proposed here exists because a stable derivative with an established metal−metal bond has been proven in the previously prepared complex $(\mathrm{Ar[}t\text{-Bu]N)_3Mo-Sn(C_6H_5)_3}$.[15]

A plausible mechanism for the reaction of **1**-H and **2** is outlined in Scheme 2. Full resolution of this kinetic scheme is beyond the scope of the current work.

Information regarding the H atom transfer step could be obtained under conditions of excess **2**, where it would be expected that $\cdot\mathrm{Mo(CO)_3(Cp)}$ produced in reaction 17 should be trapped. Under pseudo-first-order conditions of 5- to 20-fold excess **2**, plots of ln[**1**-H] versus time yielded linear plots through 2−3 half-lives. The reaction was observed to obey the rate law $\mathrm{d[P]/d}t = k_{\mathrm{obs}}[\mathbf{2}][\mathbf{1}\text{-H}]$ with $k_{\mathrm{obs}} = 0.09 \pm 0.01\ \mathrm{M^{-1}\ s^{-1}}$ at 1.3 °C and $0.26 \pm 0.04\ \mathrm{M^{-1}\ s^{-1}}$ at 17 °C. These data yield an estimate of $E_a \approx 10.7$ kcal mol^{-1} for the H atom transfer. The activation energy for binding of ligands to the sterically congested ground-state quartet metal site of **2** may make up a significant portion of this activation energy. For example, binding of AdN≡C to **2** was found to have $\Delta H^{\ddagger} = 5.5 \pm 0.5$ kcal mol^{-1}.[54] Furthermore, thermochemical estimates for the bond dissociation energy of H−Mo in both **1**-H and **2**-H discussed earlier show that the bond in **1**-H is about 4−8 kcal mol^{-1} stronger than that in **2**-H. Thus, the E_a of ∼10.7 kcal mol^{-1} is close to the sum of enthalpy of activation for bringing a ligand into the coordination sphere of **2** plus the energy difference between the two Mo−H bonds.

Comparison to studies done at 17 °C of the rate of reaction of **1**-D yielded $k_H/k_D = 1.00 \pm 0.05$ as shown in Supporting Information (Figure SF4). The low or zero kinetic isotope effect is consistent with an early transition state in which formation of the adduct $\mathrm{(Ar[}t\text{-Bu]N)_3Mo\cdots HMo(CO)_3(Cp)}$ is the rate limiting step.

The reaction of **2** and **1**-H is much slower than that observed for **2**-NCPh and **1**-H. This may be because of the greater accessibility at a site removed from the crowded metal center in the latter reaction. A similar rate acceleration was previously observed[1] for the reaction of benzoyl peroxide with **2**-NCPh compared to **2**.

Despite the abundant reports in the literature regarding hydrogen atom transfer from metal carbonyl hydrides to carbon-based radicals[46,48,49] and to olefins,[45,55] works related to hydrogen atom transfer between metal complexes[56] are

(45) More O'Ferral, R. A. *J. Chem. Soc. B* **1970**, 785.
(46) Bullock, R. M.; Samsel, E. G. *J. Am. Chem. Soc.* **1990**, *112*, 6886.
(47) Cheng, T. -Y.; Bullock, R. M. *J. Am. Chem. Soc.* **1999**, *121*, 3150.
(48) Franz, J. A.; Linehan, J. C.; Birnbaum, J. C.; Hicks, K. W.; Alnajjar, M. S. *J. Am. Chem. Soc.* **1999**, *121*, 9824.
(49) Eisenberg, D. C.; Lawrie, C. J. C.; Moody, A. E.; Norton, J. R. *J. Am. Chem. Soc.* **1991**, *113*, 4888.
(50) Huynh, M. H. V.; Meyer, T. J. *Chem. Rev.* **2007**, *107*, 5004.
(51) Mayer, J. M.; Rhile, I. J. *Biochim. Biophys. Acta* **2004**, *1655*, 51.
(52) Zdilla, M. J.; Dexheimer, J. L.; Abu-Omar, M. M. *J. Am. Chem. Soc.* **2007**, *129*, 11505.
(53) For a review comparing hydride, proton and hydrogen atom transfer reactions of metal hydrides, see: Bullock, R. M. *Comments Inorg. Chem.* **1991**, *12*, 1.
(54) Stephens, F. H.; Figueroa, J. S.; Cummins, C. C.; Kryatova, O. P.; Kryatov, S. V.; Rybak-Akimova, E. V.; McDonough, J. E.; Hoff, C. D. *Organometallics* **2004**, *23*, 3126.

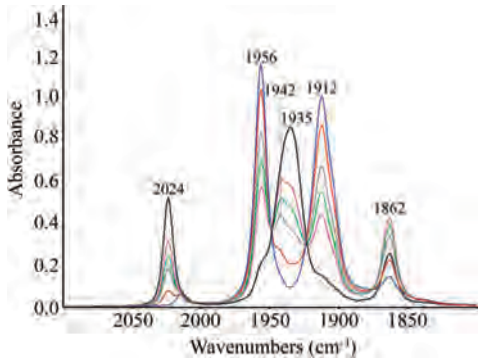

Figure 8. Reaction of **1**-H and **2**. The bands at 2024 and 1935 cm^{-1} are from the starting **1**-H; those at 2015 (w) 1956, 1912 cm^{-1} are from the final product $\mathbf{1}_2$, and an intermediate assigned as **1**−**2** has bands that rise and then shrink at 1942 and 1862 cm^{-1}. Qualitative study of the reaction products performed at room temperature over a period of three hours.

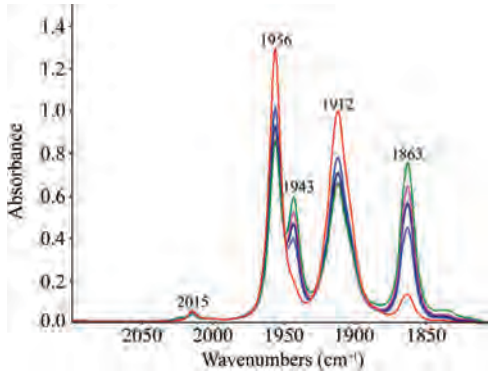

Figure 9. Reaction of **2** (0.098 M) and $\mathbf{1}_2$ (0.015 M) in toluene solution at room temperature. The bands at 1943 and 1863 cm^{-1} assigned to (Ar[*t*-Bu]N)$_3$Mo−Mo(CO)$_3$(Cp) grow with time, while those assigned to $\mathbf{1}_2$ at 2015 (w), 1956, 1912 cm^{-1} shrink. Spectra obtained starting at 2, 15, 25, 95, and 960 min.

Scheme 2. Proposed Mechanism for the Reaction of **1**-H and **2**

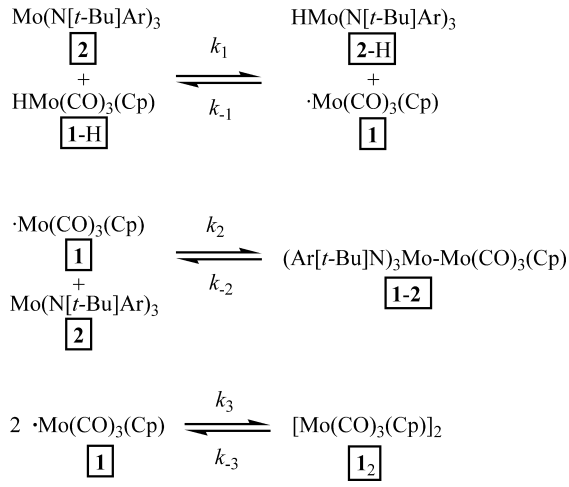

scarce, and no detailed studies of kinetic isotope effects or activation parameters could be found for comparison to our results.

Conclusions

The Mo−H bond dissociation energy in **2**-H of ∼62 kcal mol^{-1} was lower than expected on the basis of the generally strong bonds found previously for the Mo(N[*t*-Bu]Ar)$_3$ system. In contrast, the C−H bond of (Ph(**H**)**C**═N)Mo(N[*t*-Bu]Ar)$_3$ of ∼90 kcal mol^{-1} and the metal to ketimide bond strength (Ph(H)C═**N**)**Mo**(N[*t*-Bu]Ar)$_3$ of ∼71 kcal mol^{-1} are both high. The combination of these factors make benzonitrile insertion into the XMo(N[*t*-Bu]Ar)$_3$ bond thermodynamically favorable for X = H in contrast to cases where nitrile extrusion is observed (X = OC(O)Ph, TePh, SeC_6F_5, SC_6F_5).

The transfer of an H atom from **1**-H to **2** is uphill by 4−8 kcal mol^{-1}. The driving force for atom transfer is the formation of a Mo−Mo bond in the dimerization of the metal radical **1**. The reaction proceeds with initial trapping of ·Mo(CO)$_3$(Cp) by **2** to form a complex proposed as (Ar[*t*-Bu]N)$_3$Mo−Mo(CO)$_3$(Cp) which ultimately goes on to form $\mathbf{1}_2$. The rate constant for this reaction at 17 °C of 0.26 M^{-1} s^{-1} is nearly 4 orders of magnitude slower than that for the H atom transfer from **1**-H to **2**-NCPh of 1.8 × 10^3 M^{-1} s^{-1}.[57] However the reaction rate is nearly 5 orders of magnitude slower than the value of 3.9 × 10^8 M^{-1} s^{-1} for H atom transfer from **1**-H to the hex-5-enyl radical.[58]

Acknowledgment. The authors are grateful for support of this work by the National Science Foundation Grants CHE 0615743, 0719157, and 0750140, the Department of Energy Grant DE-FG02-06ER15799, and the Spanish Ministry of Education and Science and the Fulbright commission under Fellowship FU-2006-1738. Stopped-flow instrumentation at Tufts was supported by the NSF CRIF Grant (CHE-0639138). We wish to thank John J. Curley for crystallographic assistance.

Supporting Information Available: NMR spectra showing the nitrile insertion in the Mo−H bond of **2**-H, concentration dependence from **1**-H for formation of **1**-NC(Ph)H, UV−vis spectra for $\mathbf{1}_2$, **2**-NCPh, and **2**-NC(H)Ph, a complete list of all individual data obtained for k_{obs} as a function of temperature for reaction 11, and crystallographic information files (CIF). This material is available free of charge via the Internet at http://pubs.acs.org.

IC800945M

(55) Choi, J.; Tang, L.; Norton, J. R. *J. Am. Chem. Soc.* **2007**, *129*, 234, and references reported therein.
(56) (a) Nappa, M. J.; Santi, R.; Halpern, J. *Organometallics* **1985**, *4*, 34. (b) Kiss, G.; Zhang, K.; Mukerjee, S. L.; Hoff, C. D. *J. Am. Chem. Soc.* **1990**, *112*, 5657. (c) Song, J.-S.; Bullock, R. M.; Creutz, C. *J. Am. Chem. Soc.* **1991**, *113*, 9863.
(57) The value at T = 17 °C was obtained by extrapolation of data in Figure 7 of this paper.
(58) This value was extrapolated using the activation parameters reported by Franz et al, see ref 10. Data at T = 17 °C was chosen for comparison since extrapolation of data for k_1 of reaction 17 in this work based on E_a alone, was not deemed valid. The data at 17 °C are also the closest to the literature values. This comparison illustrates the wide range of H atom transfer rates from HMo(CO)$_3$(Cp).